# EVALUATION OF NEUTRON CROSS SECTIONS OF THE sd-SHELL NUCLEI $^{27}$Al AND $^{28,29,30}$Si

Hideo Kitazawa and Yoshiko Harima

Research Laboratory for Nuclear Reactors, Tokyo Institute of Technology
2-12-1 O-okayama, Meguro-ku, Tokyo 152, Japan

Tokio Fukahori

Nuclear Data Center, Japan Atomic Energy Research Institute
Tokai-mura, Naka-gun, Ibaraki-ken 319-11, Japan

Abstract: On the basis of nuclear models we have evaluated neutron cross sections of $^{27}$Al and $^{28,29,30}$Si at energies from $10^{-5}$eV to 20MeV. The model parameters, i.e. the nuclear level density parameters in the Gilbert-Cameron formula and the optical potential parameters for neutron, proton and alpha particle, were determined independently of the previous work. The calculations were mainly performed in the framework of the Hauser-Feshbach theory. However, the strong excitation of collective states by neutron inelastic scattering was fully considered with a coupled-channel Born approximation. As a result, we found that the calculations are in good agreement with recent experimental values in the whole neutron energy region.

(neutron cross section, evaluation, $^{27}$Al, $^{28,29,30}$Si, E=$10^{-5}$eV-20MeV)

## Introduction

Abundant silicon is contained in concrete which is most popularly used for neutron shielding. It is also an indispensable material of semiconductors. Therefore, neutron cross sections of the silicon nucleus are required for shielding design calculation and for radiation damage estimate. On the other hand, aluminium is in various use as a structural material. Its neutron cross sections are equally requested. In particular, the cross sections for charged-particle emission are often utilized for neutron dosimetry and as standards in neutron cross-section measurements.

In the present study, neutron cross sections of Al and Si have been calculated, employing the nuclear reaction models. However, we avoided an easy use of the model parameters which were obtained by the previous work. Rather, we intended to establish the methodology of neutron cross-section evaluation in the sd-shell nuclear region, starting from an independent determination of these parameters.

## Collective Nuclear Structure of $^{27}$Al and $^{28,29,30}$Si

In the evaluation of neutron cross sections, excitation of nuclear collective states should be accurately taken into account, because these states are strongly excited by neutron inelastic scattering.

## Structure of the $^{27}$Al

Knopfle et al./1/ have performed inelastic scattering experiments with deuterons in order to investigate the collective nuclear structure of $^{27}$Al, and found that the 5/2+ ground state, the 7/2+ (2.21MeV) state and the 9/2+ (5.43MeV) state belong to the 5/2+ ground-state rotational band. In the present study, these states were taken as members of the 5/2+ prolate ground-state rotational band. Moreover, the inelastic scattering to the 1/2+ (0.84MeV) state, the 3/2+ (1.01MeV) state and the 9/2+ (3.00MeV) state was treated by the weak coupling model, in which the 5/2+ particle state couples to the 2+ one-phonon excitation.

## Structure of $^{28,29,30}$Si

The energy states of $^{28}$Si are clearly not typical of either the simple rotational or simple vibrational model. However, Haouat et al./2/ have shown that the neutron inelastic scattering to the 0+ ground state, the 2+ (1.78MeV) state and the 4+ (4.62MeV) state is better explained by the rotational model. These states were assumed to be members of the 0+ oblate ground-state rotational band. On the $^{27}$Al(p,γ)$^{28}$Si reaction, moreover, Aleonard et al./3/ have observed the strong E3 transition from the 3- (6.88MeV) state to the ground state. Similarly, the large strength was obtained by Bister et al./4/ for the E2 transition from the 0+ (4.98MeV) state to the 2+ (1.78MeV) state. The results seem to indicate collective features of both states.

Our calculation took account of the 0+ oblate ground-state rotational band. The 0+ (4.98MeV) state was assumed to be the head of the β-vibrational band. Also, the inelastic scattering to the 3- (6.88MeV) state was described by the spherical vibrational model.

The structure of $^{29}$Si is generally well accounted for with either a band-mixed Nilsson calculation or with an intermediate core-coupling approach. In the present study, the inelastic scattering to the 5/2+ (2.03MeV) state, the 3/2+ (2.43MeV) state, the 9/2+ (4.74MeV) state and the 7/2+ (5.29MeV) state was predicted by the pure Nilsson model with an assumption of static oblate deformation. These states were considered to be members of the 1/2+ ground-state rotational band. For $^{30}$Si, we assumed the 0+ oblate ground-state rotational band, whose members are the 0+ ground state, the 2+ (2.24MeV) state and the 4+ (5.95MeV) state.

## Fundamental Nuclear Model Parameters

### Resonance Parameters

Below the 0.6MeV neutron energy, the total cross sections of $^{27}$Al were expressed with the resonance parameters. Similarly, the resonance regions of $^{28}$Si, $^{29}$Si and $^{30}$Si were taken to be below 1.9MeV, 0.1MeV and 0.5MeV neutron energy, respectively. Using the RESENDD code/5/ based on the multi-level Breit-Wigner formalism, resonance parameters were searched so as to

reproduce the observed cross sections of Larson et al./6/. Consequently we found that for the 188keV s-wave resonance the neutron width is about half of the value in BNL-325/7/. As shown in Table 1, our value is in good agreement with the evaluated value of Hermsdorf/8/.

Table 1. s-wave resonance parameters of $^{28}$Si

|  | $E_n$ (keV) | $\Gamma_n$ (keV) | $\Gamma_\gamma$ (eV) |
|---|---|---|---|
| Present | 55.6 | 0.7 | 1.5 |
|  | 180.0 | 31.0 | 9.0 |
| BNL-325 | 55.0 | 1.5 | 1.5 |
|  | 188.0 | 60.0 | 9.0 |
| Hermsdorf | 55.6 | 1.5 | 0.54 |
|  | 186.5 | 29.0 | 13.8 |

Level Density Parameters

For the nuclear level density, we adopted the Gilbert-Cameron composite formula/9/ which was derived from the constant temperature model and the Fermi gas model. The constant temperature model produces

$$\rho_1(E) = \frac{1}{T} \exp(\frac{E-E_0}{T}) \qquad (1)$$

and the Fermi gas model leads to

$$\rho_2(U) = \frac{\sqrt{\pi}}{12} \frac{\exp(2\sqrt{aU})}{a^{1/4} U^{5/4}} \frac{1}{\sqrt{2\pi}\sigma} \qquad , \qquad (2)$$

where E is the nuclear excitation energy in the reality and U is the nuclear excitation energy in the Fermi gas model. The quantities, a and T, are the level density parameter and the nuclear temperature, respectively. The spin cut-off parameter $\sigma$ was taken to be $\sigma^2 = 0.146\sqrt{aU} A^{2/3}$, and $E_0$ was defined as a characteristic energy at which the nuclear entropy is zero.

Since detailed information is available on discrete energy levels of nuclei with A≤40, T and $E_0$ are easily obtained from a cumulative plot of these energy levels. When the level information on a nucleus is scanty, the cumulative plot of its mirror nucleus is utilized. Consequently we found that the cumulative plots of all the nuclei concerned in the reactions on Al and Si are represented by the common nuclear temperature T=2.024MeV, independent of mass number and atomic number. Probably, this is due to the high degeneracy of the Fermi system. Also, we defined the pairing energy of a nucleus to be the energy shift of its cumulative plot from that of the $^{28}$Al nucleus. The reason is that this shift may be the energy needed to break the pairing correlation in the vicinity of the Fermi level.

The level density parameter a was determined so that eq. (1) connected smoothly to eq. (2) at the energy $U_x$ satisfying the equation

$$\frac{1}{T} = \sqrt{\frac{a}{U_x} - \frac{3}{2U_x}} \qquad (3)$$

Nuclear levels near the ground state can not be described by the constant temperature model, because nucleon-nucleon correlation or collective excitation is often preponderant in these nuclear states. Therefore, they were treated as discrete levels in computer programs.

Optical Potential Parameters

As a neutron optical potential in the spherical potential model, we used a modification of the potential of Whisnant et al./10/ which was obtained for $^{27}$Al above the 11MeV neutron energy. Since the real potential of Whisnant et al. overestimates the average total cross sections at lower neutron energies, the modified real potential whose depth is constant and slightly shallower below the 11MeV neutron energy was employed. Also, the surface absorption potential depth was taken to increase with neutron energy below 11MeV. This is due to the fact that the open channel increases with neutron energy. Consequently the Hauser-Feshbach model calculations using the modified potential reproduced well the energy dependence of the $^{27}$Al(n,2n)$^{26}$Al reaction cross sections/11/ near the threshold. The optical potential in the deformed potential model was taken to be that of Whisnant et al. The spherical optical potential parameters for neutron are:

V = 51.87 - 0.31E(MeV)     ( $\geq$ E = 11.0MeV )
W = 7.14MeV

V = 48.46MeV               ( $\leq$ E = 11.0MeV )
W = 4.94 + 0.20E(MeV)

$a_0$ = 0.64fm    $r_0$ = 1.18fm
$a_w$ = 0.58fm    $r_w$ = 1.26fm
$a_{s0}$ = 0.50fm    $r_{s0}$ = 1.01fm    $V_{s0}$ = 6.0MeV

The proton optical potential was assumed to be the same with the neutron potential. It is also expected from the viewpoint of the charge independence of the nuclear force. The Hauser-Feshbach calculations using this potential reproduced well the $^{27}$Al(n,p)$^{29}$Mg reaction cross sections and the emitted proton spectrum/12/ for 15MeV neutrons.(see fig.1) Our potential is rather different from the global potential of Perey et al./13/ in respect that the absorption term of the former potential increases with proton energy below 11MeV.

The global alpha-particle optical potential except for that of Huizenga and Igo/14/ is not available. In the framework of the spherical potential model, therefore, we determined the alpha-particle optical potential so as to reproduce the $^{27}$Al(n,$\alpha$)$^{24}$Na reaction cross sections, because these cross sections are often used as standards. In the calculation, only the statistical reaction process was assumed for the (n,$\alpha$) reaction, because the angular distribution of emitted alpha-particles for 14MeV neutrons is almost symmetric around 90°/15/. At the starting point of the optical potential search, we took the real potential depth of 200MeV which is about four times deeper than that of the nucleon potential. Also, we assumed the radius parameters to be larger than those of the nucleon potential, taking account of the spatial extent of the alpha particle. Using these parameters, we adjusted the depth of the surface absorption potential so as to reproduce the (n,$\alpha$) reaction cross sections and the emitted alpha-particle spectrum/12/ for 15MeV neutrons.(see fig.2) Consequently we found that the depth of the absorption potential drastically decreases under the Coulomb potential barrier (~6MeV). At present, it will be difficult to give a physical explanation for the above absorption potential. The spherical optical potential parameters for alpha particle are:

V = 200MeV
W = 0.8MeV    ( ≤ E = 6.0MeV )
  = 30.0MeV   ( 6.5MeV ≤ E ≤ 7.0MeV )
  = 40.0MeV   ( ≳ E = 7.5MeV )

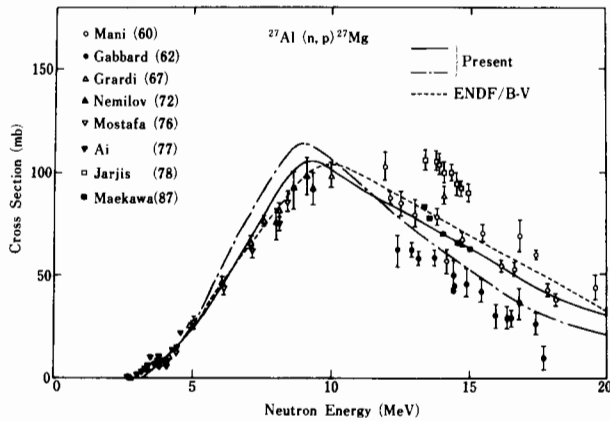$a_0$ = 0.53fm    $r_0$ = $r_c$ = 1.65fm
$a_w$ = 0.62fm    $r_w$ = 1.75fm



Fig.1 $^{27}$Al(n,p)$^{27}$Mg reaction cross sections.
The solid line was calculated using
the optical potential of our work, and
the dot-dashed line using the potential
of Perey and Perey/13/.

## Evaluation of Neutorn Cross Sections

In the model calculation, the neutron cross
section was defined as an incoherent sum of the
contributions of direct and statistical process.
Then, we took account of the flux normalization
by subtracting the cross section for direct
process from the compound-nucleus formation cross
section. The elastic scattering cross section was
taken to be the difference between the total and
reaction cross sections.

## Total Cross Sections

In the resonance region, total cross
sections were obtained from the multi-level
Breit-Wigner formula, using the resonance
parameters. In other region, they were calculated
by the CASTHY code/16/; otherwise so obtained as
to trace the experimental values.

## Neutron Capture Cross Sections

Neutron capture cross sections in the
resonance region were obtained in the same way
with the total cross section. In other region,
statistical model calculations were performed
with the CASTHY code, while direct and semi-
direct model calculations were performed with the
HIKARI code/17/ programed on the base of the
collective capture theory.

## Proton and Alpha-particle Emission Cross Sections

The cross sections and emitted particle
spectra were calculated with the GNASH code/18/,
using the model parameters obtained in the
present study. However, since the $^{27}$Al(n,$\alpha$)$^{24}$Na
reaction cross sections are standards of the
neutron cross section, we adopted as the data of
JENDL-3 the cross sections which were obtained by
a least-square fitting to the observed values.

## Neutron Scattering Cross Sections

The statistical model calculations were
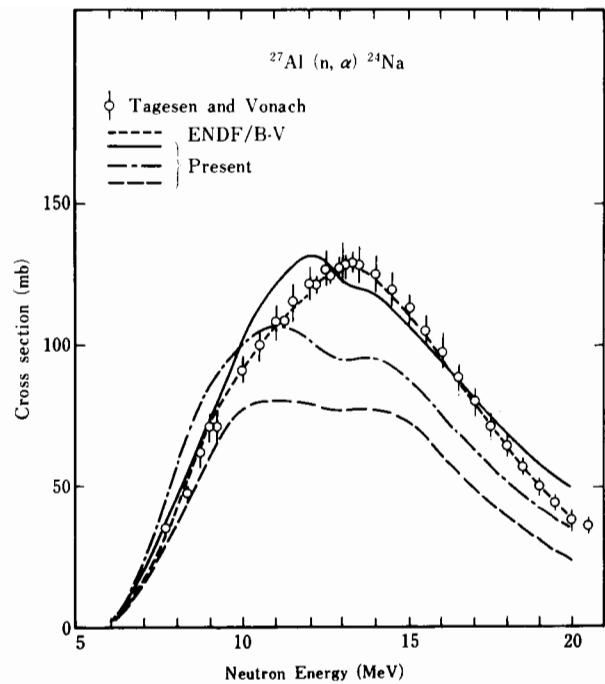performed with the CASTHY code, taking account of



Fig.2 $^{27}$Al(n,$\alpha$)$^{24}$Na reaction cross sections.
The solid, dot-dashed and dashed lines
were calculated using the alpha-particle
potential parameters of our work,
Huizenga and Igo/14/ and Lemos /22/,
respectively.

the width fluctuation. The scattering to the
ground state rotational band of $^{27}$Al was
calculated by the ECIS code/19/. The deformation
parameters were taken to be $\beta_2$=0.34 and $\beta_4$=0.
Also, we calculated the direct excitation of the
1/2+ (0.84MeV), 3/2+ (1.01MeV) and 9/2+ (3.00MeV)
states by the JUPITOR-1 code/20/, assuming the
weak coupling between the 5/2+ particle state and
the 2+ one-phonon state (coupling constant
=0.45). The results are in excellent agreement
with the experimental values of Whisnant et al.,
except for the 0.84MeV and 1.01MeV states.

The scattering to the ground rotational band
of $^{28}$Si was calculated by the ECIS code, using
the deformation parameters, $\beta_2$=-0.39 and $\beta_4$=0.24.
The direct excitation of the 3- (6.88MeV) state
was calculated by the spherical vibrational
model, using the ECIS code and taking the
deformation parameter $\beta_3$=0.3. The direct
excitation of the 0+ (4.98MeV) state was
predicted by the JUPITOR-1 code, assuming that
this state is the head of the $\beta$-vibrational band.
The deformation parameter $\beta_2$ was taken to be -
0.39, and the coupling constant between the
ground state and the $\beta$-vibration to be 0.22. The
calculations are in excellent agreement with the
observed values of Haouat et al./2/ and Seeliger
et al/21/. Moreover, it was confirmed that in the
coupled channel Born approximation the complex
coupling produces better results than the real
coupling. (see fig. 3)

## Neutron and Gamma-ray Production Cross Sections

Using the above results, we calculated
neutron and gamma-ray production cross sections
by the GNASH code. Here, the E1 gamma-ray
strength with the Brink-Axel profile function was
determined, using the E1 sum rule and the level
distance calculated from the level density
parameter. As examples, comparison between the

calculated and observed values is given in figs. 4 and 5. An overall agreement between both results is excellent.
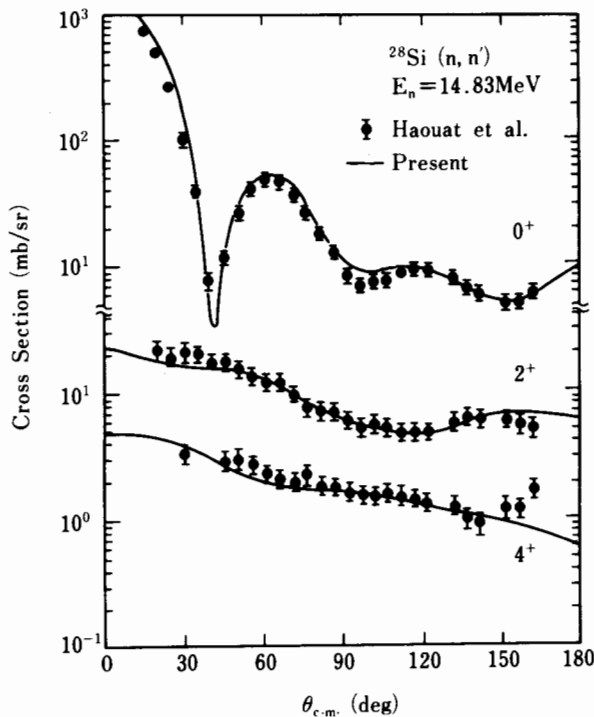


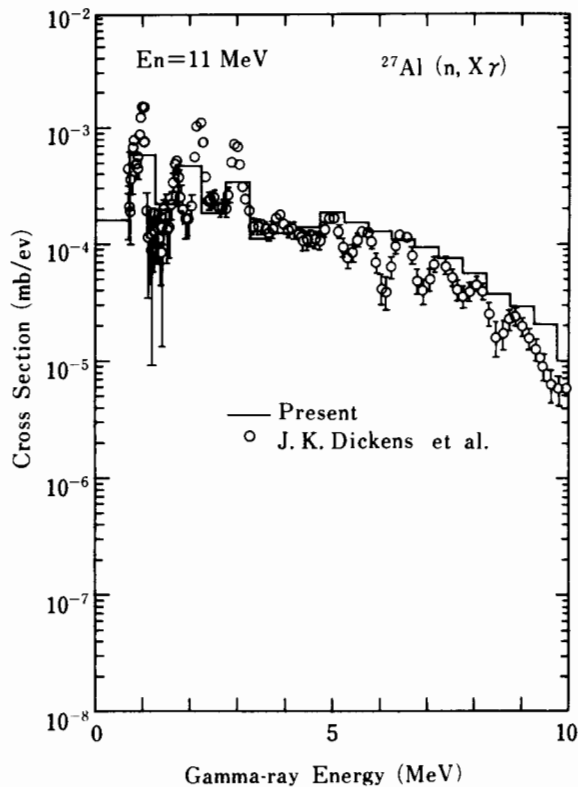Fig.3 Neutron scattering of 14.8MeV neutron by $^{28}$Si



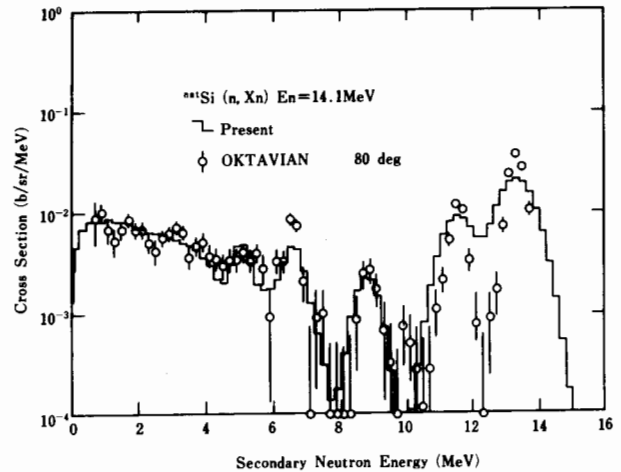Fig.4 Gamma-ray production cross sections of $^{27}$Al at the 11MeV neutron energy.



Fig.5 Neutron emission cross sections of $^{nat}$Si at the 14.1MeV neutron energy.

## Summary

In the present study, we found that lower excited states of the nuclei concerned in neutron reactions on $^{27}$Al and $^{28,29,30}$Si are succesfully described by the constant temperature model including only one common nuclear temperature. Moreover, the optical potential parameters were so taken as to include the dependence of the real and imaginary potential depths on particle energy. Particularly, the depth of the absorption potential for alpha particle decreases drastically under the Coulomb potential barrier. Using these parameters, the model calculations in the framework of the Hauser-Feshbach theory and the coupled-channel Born approximation produced the neutron cross sections in good agreement with experimental data at the energies from $10^{-5}$ eV to 20MeV

## REFERENCES

1. K.T. Knöpfle et al: Phys.Rev. C13,1400(1976)
2. G. Haouat et al: Phys.Rev. C30,1795(1984)
3. M.M. Aleonard et al: Nucl.Phys.A146,90(1970)
4. M. Bister et al: Can.J.Phys. 47,2539(1969)
5. T. Nakagawa: JAERI-M, 84-192(1984)
6. D.C. Larson et al: ORNL-TM-5618(1976)
7. S.F. Mughabghab et al: Neutron Cross Sections, Vol.1(1981)
8. D. Hermsdorf: INDC(GDR)-20(1982)
9. A. Gilbert and A.G.N. Cameron: Can. J. Phys. 43, 1446(1965)
10. C.S. Whisnant et al: Phys.Rev.C30,1435(1984)
11. S. Iwasaki et al: Annual Research Report of Japanese Contributions for Japan-US Collaboration on RTNS-II Utilization(1987)
12. S.M. Grimes et al: Nucl.Sci.Eng.62,187(1977)
13. C.M. Perey and F.G. Perey: Atomic data Nucl. Data Tables 17, 1(1976)
14. J.R. Huizenga and G. Igo: Nucl. Phys. 29, 462(1962)
15. U. Seebedk and M. Bormann: Nucl. Phys. 68, 387(1965)
16. S. Igarasi: J.Nucl.Sci.Technol. 12, 67(1975)
17. H. Kitazawa: private communication
18. P.G. Young and E.D. Arthur: LA-6947(1977)
19. J. Raynal: coupled channel code ECIS79(1979)
20. T. Tamura: ORNL-4152(1967)
21. D. Seeliger et al: Nucl.Phys.A460,265(1986)
22. O.F. Lemos: ORSAY, SERIE A, No. 136(1972)